Generation and dynamics of phononic cat states after optical excitation of a quantum dot

D. E. Reiter,[1] D. Wigger,[1] V. M. Axt,[2] and T. Kuhn[1]

[1]*Institut für Festkörpertheorie, Universität Münster, Wilhelm-Klemm-Strasse 10, D-48149 Münster, Germany*

[2]*Theoretische Physik III, Universität Bayreuth, D-95440 Bayreuth, Germany*

(Received 25 July 2011; revised manuscript received 4 November 2011; published 28 November 2011)

We study theoretically the fluctuation properties of optical phonons generated after optical excitation of a quantum dot. If the quantum dot exciton is optically manipulated by ultrafast laser pulses, the electronic system and the phonon system can become entangled, which strongly influences the fluctuation properties of the phonons. When reduced to the phonon system, such an entanglement corresponds to a mixed phonon state. We discuss excitations with one or two ultrafast laser pulses. For a single pulse excitation, in general, a statistical mixture of two coherent states is found. For more pulses, a statistical mixture of superpositions of coherent states builds up in the phonon system. With the help of the Wigner function, which provides an intuitive picture of the generated phonon states, we explain how these states are formed depending on the excitation conditions and illustrate their time evolution. From this the fluctuation properties of the corresponding states can be well interpreted and the conditions for obtaining phonon squeezing are identified.

DOI: 10.1103/PhysRevB.84.195327 PACS number(s): 43.35.Gk, 63.20.kd, 42.50.Dv, 78.67.Hc

I. INTRODUCTION

Nonclassical phonon states have attracted increasing interest in the past few years. In particular, the search for squeezed phonon states has been the focus of various experimental and theoretical investigations.[1–8] Phonons are in many aspects similar to photons, where squeezing has been extensively studied in the past.[9] However, for phonons, a direct measurement of the fluctuation properties seems rather complicated and, thus, only more or less indirect hints for squeezed phonons were found. One of the indications of phonon squeezing was the observation of an oscillation of the lattice fluctuations with twice the phonon frequency.[1–5] However, such an oscillation turned out not to be an unambiguous proof for squeezing.[8,10]

Squeezing can be achieved in different ways. One way is to deform ("squeeze") the vacuum or a coherent state in phase-space representation. Mathematically, this can be performed by a squeezing operator acting on the vacuum or coherent state.[11,12] A physical realization in the case of photons is given by the parametric downconversion in a nonlinear-optical crystal.[11] An analogous process for phonons is the anharmonic decay of an optical phonon into a pair of acoustic phonons, which may lead to squeezed states of acoustic phonons.[7,13] A similar squeezing mechanism is provided by a second order Raman process which can also be described in terms of a squeezing operator.[4,6,14]

An alternative way to achieve squeezing is to create a superposition of two (or more) coherent states.[11,12,15,16] Such states are generally called cat states[11,12] and prominent examples are the even and odd coherent states[17] or the Yurke-Stoler states.[18] In a cat state, through the action of quantum interference, the fluctuations can be reduced below the value of the fluctuations of the coherent or vacuum state and, thus, squeezing can occur. Cat states in other systems have been extensively studied experimentally and theoretically, e.g., with ultracold atoms[19] or photons.[20] In this paper we study the generation and dynamics of phononic cat states in a semiconductor system, which can lead to phonon squeezing as we have shown recently.[10] The specific phonon state is not created directly by the ultrafast optical excitation but indirectly via the generation and manipulation of the quantum dot exciton. This indirect generation mechanism is fundamentally different from the generation of phonon squeezing as described by a squeezing operator in the Raman model.[4,6,7] The optical excitation leads to an entanglement between electrons and phonons in the quantum dot and, thus, when reduced to the phonon degrees of freedom, to a mixed phonon state. As a consequence, in the case of a two-pulse excitation, not a single cat state is created; instead, a statistical mixture of two cat states builds up, each of them consisting of a superposition of two coherent states. It turns out that the occurrence of phonon squeezing depends on many parameters that characterize the semiconductor structure as well as the excitation conditions.

In this paper we present a detailed analysis of the generated phonon states in an optically excited quantum dot structure depending on the excitation conditions. We will show that the Wigner representation of the phonon state provides a very useful concept to obtain an intuitive understanding of the light-pulse-induced phonon dynamics. While for coherent or thermal phonon states the Wigner function is strictly positive, quantum interference may give rise to negative values. Such negative values are clear indications of nonclassical states. We will show that, indeed, in a certain range of excitation parameters these negative values in the Wigner function are associated with phonon squeezing.

The paper is organized as follows. In Sec. II we describe the theoretical model of the quantum dot coupled to the light field and phonons, we define the relevant dynamical variables for the phonon system, and we introduce the Wigner function. Section III contains the results and detailed discussion of the phonon states generated by a single pulse (Sec. III A) and by a double pulse (Sec. III B) excitation. The paper finishes in Sec. IV with some concluding remarks.

II. MODEL SYSTEM

To be specific, we consider a spherical semiconductor quantum dot, which we model as a two-level system consisting of the ground state $|g\rangle$ and the lowest exciton state $|x\rangle$. This is

a valid approximation in the strong confinement limit, where excited exciton states are sufficiently separated from the lowest exciton state, and in the case of excitation by circular light pulses where the generation of biexcitons is prohibited. The coupling to the phonons is modeled by pure dephasing-type interactions, as described in the independent Boson model. In the case of coupling to acoustic phonons, the independent Boson model has been shown to quantitatively reproduce the experimentally observed nonexponential polarization decay behavior on short time scales.[21] Here we will concentrate on the coupling to longitudinal optical (LO) phonons, which we assume to be dispersionless with the frequency ω_0 and a corresponding period $t_0 = 2\pi/\omega_0$. LO phonons are spectrally well separated from acoustic phonons and, because of their characteristic frequency, signatures of their dynamics are typically easier to observe. The interaction between exciton and LO phonons is described by the standard Fröhlich coupling. The coupling of the electronic states to the electric field of the laser is treated in dipole and rotating wave approximation. We assume an excitation by ultrashort pulses, which we model mathematically by δ pulses. Physically, in order to generate coherent phonons, the pulse has to be short compared to the phonon oscillation period t_0. Indeed, experiments with pulse lengths of few tens of fs have successfully been shown to create coherent phonons.[22–25] The present model has the big advantage that it allows for an analytical solution under the excitation by an arbitrary sequence of such ultrafast laser pulses.[26,27]

Within this model, the Hamiltonian of the whole system reads

$$\hat{H} = \hbar\left[\Omega + \sum_{\mathbf{q}}(g_{\mathbf{q}}\,\hat{b}_{\mathbf{q}} + g^*_{\mathbf{q}}\,\hat{b}^\dagger_{\mathbf{q}})\right]|x\rangle\langle x| + \hbar\omega_0\sum_{\mathbf{q}}\hat{b}^\dagger_{\mathbf{q}}\hat{b}_{\mathbf{q}} - \hat{\mathbf{P}}\cdot\mathbf{E}, \tag{1}$$

with the exciton energy $\hbar\Omega$, $\hat{b}_{\mathbf{q}}$ ($\hat{b}^\dagger_{\mathbf{q}}$) is the annihilation (creation) operator of a LO phonon with wave vector $\mathbf{q}$, $g_{\mathbf{q}}$ is the carrier-phonon coupling matrix element, $\mathbf{E}$ is the laser field, and $\hat{\mathbf{P}} = \mathbf{M}_0|x\rangle\langle g| + \mathbf{M}^*_0|g\rangle\langle x|$ is the operator for the electronic polarization with the transition dipole matrix element $\mathbf{M}_0$. A suitable basis for the description of the total system is provided by $|X; ph\rangle$, which are product states of the electronic states $|X\rangle \in \{|g\rangle, |x\rangle\}$ and the phonon states $|ph\rangle$.

The annihilation and creation operators for the LO phonons lead to the lattice displacement

$$\hat{\tilde{\mathbf{u}}}(\mathbf{r},t) = -\frac{iu_0}{\sqrt{N}}\sum_{\mathbf{q}}\frac{\mathbf{q}}{q}(\hat{b}_{\mathbf{q}}e^{i\mathbf{q}\cdot\mathbf{r}} - \hat{b}^\dagger_{\mathbf{q}}e^{-i\mathbf{q}\cdot\mathbf{r}}), \tag{2}$$

and its conjugate variable, the momentum

$$\hat{\tilde{\pi}}(\mathbf{r},t) = -\frac{\pi_0}{\sqrt{N}}\sum_{\mathbf{q}}\frac{\mathbf{q}}{q}(\hat{b}_{\mathbf{q}}e^{i\mathbf{q}\cdot\mathbf{r}} + \hat{b}^\dagger_{\mathbf{q}}e^{-i\mathbf{q}\cdot\mathbf{r}}), \tag{3}$$

with $u_0 = \sqrt{\hbar/(2M_r\omega_0)}$ and $\pi_0 = \sqrt{(\hbar M_r\omega_0)/2}$. M_r is the reduced mass of the lattice ions. The quantities $\hat{\tilde{\mathbf{u}}}(\mathbf{r},t)$ and $\hat{\tilde{\pi}}(\mathbf{r},t)$ are the observables in the system. In the following we will consider the normalized, dimensionless operators given by

$$\hat{\mathbf{u}} = \hat{\tilde{\mathbf{u}}}/u_0, \quad \hat{\pi} = \hat{\tilde{\pi}}/\pi_0. \tag{4}$$

We are interested in the fluctuations of these variables, which are defined as

$$[\Delta u(\mathbf{r},t)]^2 = \langle\hat{\mathbf{u}}(\mathbf{r},t)\cdot\hat{\mathbf{u}}(\mathbf{r},t)\rangle - \langle\hat{\mathbf{u}}(\mathbf{r},t)\rangle^2 \tag{5}$$

and analogously for the momentum. Because the quantum dot has spherical symmetry, both expectation values and fluctuations only depend on the radial coordinate.

In the Hamiltonian of Eq. (1), the exciton is coupled to an infinite number of phonon modes. However, for dispersionless phonons, the Hamiltonian can be transformed to a new set of phonon modes $\hat{B}_\lambda$ and $\hat{B}^\dagger_\lambda$ by the unitary transformation[28]

$$\hat{B}_\lambda = \sum_{\mathbf{q}}\alpha^\lambda_{\mathbf{q}}\hat{b}_{\mathbf{q}}, \quad \hat{B}^\dagger_\lambda = \sum_{\mathbf{q}}\alpha^{\lambda*}_{\mathbf{q}}\hat{b}^\dagger_{\mathbf{q}}. \tag{6}$$

If we now choose one coupling element, say for $\lambda = 0$, to $\alpha^0_{\mathbf{q}} = g_{\mathbf{q}}/G$ with $G = \sqrt{\sum_{\mathbf{q}}|g_{\mathbf{q}}|^2}$, we find that in the transformed Hamiltonian, only B_0 couples to the excitonic system with the new coupling constant G:

$$\hat{H} = \hbar[\Omega + G\,(\hat{B}_0 + \hat{B}^\dagger_0)]|x\rangle\langle x| + \hbar\omega_0\sum_\lambda\hat{B}^\dagger_\lambda\hat{B}_\lambda - \hat{\mathbf{P}}\cdot\mathbf{E}\,. \tag{7}$$

All other modes $\lambda \neq 0$ do not couple to the two-level system and remain in their initial state, which in our case will be the vacuum state.

When we consider the case without laser field and restrict ourselves to the phonon mode B_0, the Hamiltonian from Eq. (7) can be easily diagonalized by introducing a linear shift for the phonon mode

$$\hat{\tilde{B}}_0 = \hat{B}_0 + \Gamma|x\rangle\langle x| = \hat{T}(\Gamma)\hat{B}_0, \tag{8}$$

$$\hat{\tilde{B}}^\dagger_0 = \hat{B}^\dagger_0 + \Gamma|x\rangle\langle x| = \hat{T}(\Gamma)\hat{B}^\dagger_0, \tag{9}$$

with $\Gamma = G/\omega_0$. Formally, this linear shift can be written as the action of a shift operator $\hat{T}(\Gamma)$. In this case, the Hamiltonian takes the simple form

$$\hat{\tilde{H}} = \hbar\tilde{\Omega}|x\rangle\langle x| + \hbar\omega_0\hat{\tilde{B}}^\dagger_0\hat{\tilde{B}}_0, \tag{10}$$

with the polaron-shifted exciton energy

$$\hbar\tilde{\Omega} = \hbar\Omega + \frac{G^2}{\omega_0}. \tag{11}$$

Within the new phonon modes $\hat{B}_\lambda$, all quantities can be well defined in the transformed, unshifted system described by Eq. (7). The new variables are directly connected to the observables from Eq. (5), namely the lattice displacement and the momentum. Defining the new operator

$$\hat{U} = \hat{B}_0 + \hat{B}^\dagger_0, \tag{12}$$

the expectation value and the variance of the lattice displacement can be obtained from

$$\langle u\rangle = \frac{1}{\Gamma}I(r)\langle U\rangle, \quad \langle u^2\rangle = \frac{1}{\Gamma^2}I^2(r)(\langle U^2\rangle - 1) + 1, \tag{13}$$

with

$$I(r) = -\frac{i}{\sqrt{N}}\sum_{\mathbf{q}}\frac{\mathbf{q}\cdot\mathbf{r}}{qr}\frac{g^*_{\mathbf{q}}}{\omega_0}e^{i\mathbf{q}\cdot\mathbf{r}}. \tag{14}$$

Analogously, the operator $\hat{\Pi} = i(\hat{B}_0 - \hat{B}_0^\dagger)$ can be defined, which is connected to the momentum.

The aim of this paper is to analyze the fluctuation properties of the phonons. In particular, we are interested in the question under which conditions the phonons exhibit squeezing. Squeezing occurs when the fluctuations of one of two conjugate variables are below the corresponding vacuum fluctuations, e.g.,

$$(\Delta u)^2 < (\Delta u)^2_{\rm vac} \quad \text{or} \quad (\Delta U)^2 < (\Delta U)^2_{\rm vac}. \tag{15}$$

This condition is also referred to as vacuum squeezing, in contrast to thermal squeezing where only a reduction below the fluctuations of a thermal phonon state is required. Since here we will only consider the zero temperature limit, vacuum squeezing and thermal squeezing agree.

In order to identify squeezing in our system we introduce as new variables the normalized expectation value of the displacement,

$$E_u = \frac{\langle u \rangle}{|I(r)|} = \frac{\langle U \rangle}{\Gamma}, \tag{16}$$

and the excitation-induced fluctuations (EIF) of the displacement,

$$S_u = \frac{(\Delta u)^2 - (\Delta u)^2_{\rm vac}}{|I(r)|^2} = \frac{(\Delta U)^2 - 1}{\Gamma^2}. \tag{17}$$

Correspondingly, for the momentum π the variables E_π and S_π are defined. These variables turn out to be well suited to interpret the results, because negative values of S_u or S_π directly indicate the presence of squeezing in the respective variable.[10]

To illustrate and interpret the results we will use the Wigner function defined by[12]

$$W(U,\Pi) = \frac{1}{4\pi} \int_{-\infty}^{\infty} dX e^{-i\frac{\Pi X}{2}} \left\langle U + \frac{1}{2}X|\hat{\rho}|U - \frac{1}{2}X \right\rangle. \tag{18}$$

In the case of a pure state, the density operator is $\hat{\rho} = |\Psi\rangle\langle\Psi|$. Then the Wigner function can be calculated in position space with the wave function $\Psi(U)$ by the integral

$$W(U,\Pi) = \frac{1}{4\pi} \int_{-\infty}^{\infty} dX e^{-i\frac{\Pi X}{2}} \Psi\left(U + \frac{X}{2}\right) \Psi^*\left(U - \frac{X}{2}\right). \tag{19}$$

The Wigner function is the quantum mechanical analog to a classical distribution function. In contrast to the latter, however, the Wigner function can take negative values, typically indicating genuine quantum mechanical features like quantum interference. From the Wigner function, the probability distributions $P(U)$ and $P(\Pi)$ are obtained by integrating over the other variable:

$$P(U) = \int W(U,\Pi)\, d\Pi, \tag{20}$$

$$P(\Pi) = \int W(U,\Pi)\, dU. \tag{21}$$

With the probability distributions $P(U)$ and $P(\Pi)$, all relevant quantities $\langle U \rangle$, $\langle U^2 \rangle$, $\langle \Pi \rangle$, $\langle \Pi^2 \rangle$, the variances $\Delta U = \sqrt{\langle U^2 \rangle - \langle U \rangle^2}$, $\Delta \Pi = \sqrt{\langle \Pi^2 \rangle - \langle \Pi \rangle^2}$, and, finally, E_i and S_i, can be calculated in the standard way.[29]

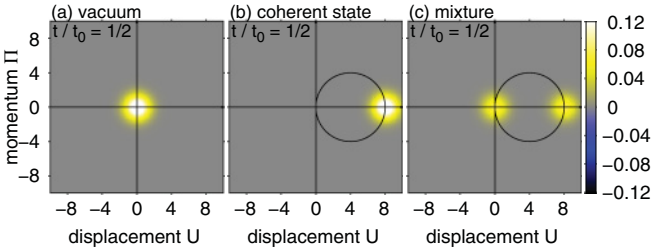

FIG. 1. (Color online) Snapshots of the Wigner function for (a) the vacuum state W_0, (b) the coherent state $W_{\beta(t)}$, and (c) the statistical mixture $W_{1\rm pulse}$ at time $t/t_0 = 1/2$ for a coupling strength of $\Gamma = 2$. The circle marks the movement of the peak position of $W_{\beta(t)}$ in time.

The Wigner function can also be calculated from its characteristic function $C(\alpha) = {\rm Tr}(\hat{\rho} e^{\alpha \hat{B}_0^\dagger - \alpha^* \hat{B}_0})$ with α being a complex number.[11] The characteristic functions are already contained in the generating functions, which have been used in previous work to calculate analytically the phonon dynamics.[21,26,27] From the characteristic function, the Wigner function is obtained by the integral

$$W(U,\Pi) = \frac{1}{\pi^2} \int d^2\alpha e^{\alpha^*(U+i\Pi) - \alpha(U-i\Pi)} C(\alpha). \tag{22}$$

The phonon vacuum gives the reference value for the fluctuations. The vacuum state is a special type of a coherent state; its wave function is given by $\Psi(U) = \exp(-U^2/4)/[(2\pi)^{1/4}]$. The corresponding Wigner function $W_0(U,\Pi)$ is a two-dimensional Gaussian around the mean $(\bar{U},\bar{\Pi}) = (0,0)$ with variances of 1:

$$W_0(U,\Pi) = \frac{1}{2\pi} \exp\left[-\frac{1}{2}(U^2 + \Pi^2)\right]. \tag{23}$$

It is shown in Fig. 1(a). Of course, in the vacuum state, the EIF S_u and S_π are zero for all times.

The generation of phonons and, as we will see, also the degree of squeezing in the generated phonon states strongly depends on the exciton-phonon coupling strength Γ. In the case of Fröhlich coupling considered here, the coupling strength is strongly influenced by the spatial overlap of electron and hole wave functions. For an exact overlap there would be no coupling at all. For example, assuming equal harmonic confinement potentials of electrons and holes, for a spherical quantum dot of 5-nm diameter and using standard GaAs material parameters, we obtain $\Gamma \approx 0.03$.[30] If electrons and holes are separated, e.g., by an in-plane electric field as discussed in Ref. 31, this value is increased by about one order of magnitude ($\Gamma \approx 0.3$). For a core-shell quantum dot made of II–VI materials as the one studied in Ref. 32 we obtain $\Gamma \approx 0.8$. In this paper we will mainly show results for a rather strong coupling ($\Gamma = 2$) because this is most instructive to interpret the quantum dynamics and compare these with the case of an intermediate value ($\Gamma = 0.5$), which turned out to be most favorable for squeezing.[10] Nevertheless, we want to mention that squeezing is also present for much smaller coupling strengths.

III. RESULTS AND DISCUSSION

A. Single pulse excitation

Let us now come to the analysis of the LO phonon dynamics following the ultrafast optical excitation of a quantum dot. It should be noted that the phonon generation is a two-step process: first the excitonic system is excited; then the charge separation associated with the exciton generation acts on the lattice ions and drives the phonon system out of its equilibrium state. The most simple case is the excitation with a single pulse with pulse area A and phase ϕ arriving at time $t = 0$. Initially, the phonon system is taken to be in its vacuum state $|0\rangle$. In the most general case, the laser pulse excites the excitonic system into a superposition of ground and exciton state, while the phonon system still remains in the ground state during the pulse. Thus, immediately after the excitation at time $t = 0^+$, the wave function reads

$$|\psi(0^+)\rangle = \cos\left(\frac{A}{2}\right)|g,0\rangle + i\sin\left(\frac{A}{2}\right)e^{i\phi}|x,0\rangle. \quad (24)$$

While the ground state does not couple to the phonon system, the exciton generation leads to the creation of phonons. The sudden creation of the exciton leads to an abrupt shift of the equilibrium position of the lattice ions. In other words, the phonon system experiences a sudden shift of the equilibrium position of its harmonic oscillator potential. Such a shift leads to the creation of a coherent state.

Let us first consider the case when the exciton is fully excited, which holds for a pulse area of $A = (2n+1)\pi$. Then the Hamiltonian in the shifted system can be diagonalized as shown in Eq. (10) and the phonons are in a coherent state $|-\tilde{\beta}(t)\rangle = |-\Gamma e^{-i\omega_0 t}\rangle$. This coherent state is an eigenstate of the annihilation operator in the shifted system

$$\hat{\tilde{B}}|\tilde{\beta}(t)\rangle = \tilde{\beta}(t)|\tilde{\beta}(t)\rangle. \quad (25)$$

Formally, it is created by the application of the displacement operator,

$$\hat{D}[\tilde{\beta}(t)] = e^{\tilde{\beta}\hat{\tilde{B}}_0^\dagger - \tilde{\beta}^*\hat{\tilde{B}}_0}, \quad (26)$$

acting on the shifted ground state $|\tilde{0}\rangle$,

$$|\tilde{\beta}(t)\rangle = D[\tilde{\beta}(t)]|\tilde{0}\rangle. \quad (27)$$

In this system the amplitude of the coherent state $|\tilde{\beta}|$ is determined by the coupling constant Γ. The initial state immediately after the pulse, i.e., the ground state in the unshifted system, is given by $|-\tilde{\beta}(0)\rangle = |-\Gamma\rangle$. By using the shift operator $\hat{T}(\Gamma)$, the coherent state is transformed back into the unshifted system:

$$\begin{aligned}|\beta(t)\rangle &= \hat{T}(\Gamma)\hat{D}[-\tilde{\beta}(t)]|\tilde{0}\rangle \\ &= e^{-i\Gamma^2\sin(\omega_0 t)}\hat{D}[\Gamma - \tilde{\beta}(t)]|0\rangle. \end{aligned} \quad (28)$$

The Wigner function for the coherent state is a two-dimensional Gaussian:[29]

$$\begin{aligned}W_{\beta(t)}(U,\Pi) = \frac{1}{2\pi}\exp\left\{-\frac{1}{2}\Big[U - 2\Gamma(1-\cos(\omega_0 t))\Big]^2\right\} \\ \times\exp\left\{-\frac{1}{2}\Big[\Pi - 2\Gamma\sin(\omega_0 t)\Big]^2\right\}. \end{aligned} \quad (29)$$

Its peak position, which corresponds to the mean values of position and momentum, moves in phase space on a circle $(\langle U\rangle,\langle\Pi\rangle) = \{2\Gamma[1-\cos(\omega_0 t)], 2\Gamma\sin(\omega_0 t)\}$ around the center $(\bar{U},\bar{\Pi}) = (2\Gamma,0)$. A snapshot of the Wigner function at the time $t/t_0 = 1/2$ is shown in Fig. 1(b) for $\Gamma = 2$. The peak position of the Wigner function moves on the indicated circle with the center (4,0). However, the shape of the Gaussian agrees with the vacuum Wigner function at any time and thus its variances are 1 for all times. Accordingly, the EIF S_u and S_π are zero for all times, as it is expected for a coherent state.

Now we consider the time evolution of the system for an arbitrary pulse area A. In this case the state $|\psi(t)\rangle$ reads

$$|\psi(t)\rangle = \cos\left(\frac{A}{2}\right)|g,0\rangle + i\sin\left(\frac{A}{2}\right)e^{i(\phi-\tilde{\Omega}t)}|x,\beta(t)\rangle, \quad (30)$$

with $\tilde{\Omega} = \Omega + \omega_0\Gamma^2$ denoting the exciton energy renormalized by the electron-phonon interaction. Obviously, as a result of the excitation the electronic and the phononic system have become entangled. Here we are only interested in the phonon dynamics, thus, we can introduce the reduced phonon density matrix obtained by tracing the full density matrix over the electronic degrees of freedom:

$$\begin{aligned}\hat{\rho}_{ph}(t) &= \mathrm{Tr}_X(|\psi\rangle\langle\psi|) \\ &= \cos^2\left(\frac{A}{2}\right)|0\rangle\langle 0| + \sin^2\left(\frac{A}{2}\right)|\beta(t)\rangle\langle\beta(t)|. \end{aligned} \quad (31)$$

Because of the entanglement, in the phononic system a statistical mixture of the phonon ground state $|0\rangle$ and the coherent state $|\beta(t)\rangle$ shows up. In this case the Wigner function $W_{1\mathrm{pulse}}(U,\Pi)$ is the sum of the Wigner functions for the ground state W_0 and for the coherent state $W_{\beta(t)}$:

$$W_{1\mathrm{pulse}} = \cos^2\left(\frac{A}{2}\right)W_0 + \sin^2\left(\frac{A}{2}\right)W_{\beta(t)}. \quad (32)$$

For a pulse area of $A = \pi/2$ the two parts of the Wigner function have equal weights with $\cos^2(\frac{A}{2}) = \sin^2(\frac{A}{2}) = 1/2$. Figure 1(c) shows a snapshot of the Wigner function $W_{1\mathrm{pulse}}(U,\Pi)$ at time $t/t_0 = 1/2$ for $\Gamma = 2$. We clearly see the two Gaussians: W_0 in the coordinate center, representing the ground state, and $W_{\beta(t)}$ moving on the indicated circle, representing the coherent state.

From the Wigner function, the probability distributions $P(U)$ and $P(\Pi)$ are extracted and shown in Fig. 2(a) as functions of time. At $t = 0$ both the vacuum state and the coherent state are located at the origin, thus, the distribution function exhibits a single peak around $U = 0$. As the vacuum state stays in the origin, a peak at $U = 0$ is observed for all times. The coherent state starts oscillating in time and correspondingly the peak in the distribution function exhibits a sinusoidal time dependence. At $t/t_0 = 1/2$, both peaks have their largest distance with respect to each other.

The probability distribution leads directly to the EIF shown in Fig. 2(b). The EIF of the lattice displacement S_u are oscillating in time. At $t = 0$ the peaks in the probability distribution coincide and thus $S_u = S_{\mathrm{vac}} = 0$. When the peak

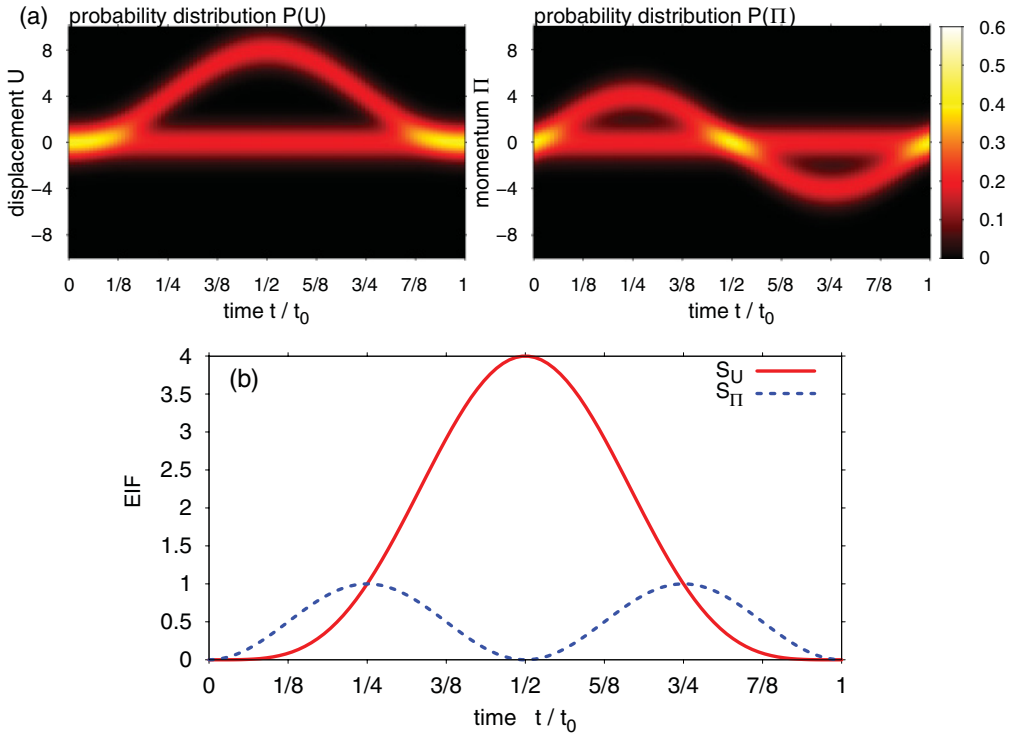

FIG. 2. (Color online) (a) Contour plot of the probability distributions $P(U)$ and $P(\Pi)$ as functions of time. (b) EIF S_u and S_π as functions of time. The coupling strength is $\Gamma = 2$.

of the coherent state moves away from the vacuum peak we see that the EIF increase reaching its maximum at $t/t_0 = 1/2$. The temporal behavior of the probability distributions shows that indeed for all times the EIF are positive with

$$(S_u)_{1\text{pulse}} = [\cos(\omega_0 t) - 1]^2 \geqslant 0.$$

The behavior of the momentum can be understood in the same way. At $t/t_0 = 0, 1/2$, and 1 the probability distributions for vacuum and coherent state coincide, thus, the excitation-induced fluctuations are zero. At $t/t_0 = 1/4, 3/4$, the distance between the Gaussians and, thus, the fluctuations are maximal. In summary, also EIF of the momentum are always positive with

$$(S_\pi)_{1\text{pulse}} = [\sin(\omega_0 t)]^2 \geqslant 0.$$

As pointed out in previous studies,[10,29] the fluctuations of the phonon state oscillate with both the single and double phonon frequency though showing no squeezing. Thus, while neither the vacuum nor the coherent state showed a time-dependent fluctuation, in the statistical mixture of the vacuum state and a coherent state, the EIF are time-dependent and oscillating with the single and double phonon frequency.

B. Two-pulse excitation

In the next step we will study the case of excitation with two ultrafast laser pulses, the first one arriving at $t = -\tau$ with pulse area A_1 and phase ϕ_1 and the second one at $t = 0$ with pulse area A_2 and phase ϕ_2. Immediately after the second pulse, at time $t = 0^+$, the system is in the state

$$\begin{aligned}|\psi(0^+)\rangle &= K_1(K_2|g\rangle + iS_2 e^{i\phi_2}|x\rangle)|0\rangle \\ &\quad + iS_1 e^{i\phi_1}(K_2|x\rangle + iS_2 e^{-i\phi_2}|g\rangle)|\beta(\tau)\rangle, \end{aligned} \tag{33}$$

where we have introduced the abbreviations $K_i = \cos(A_i/2)$ and $S_i = \sin(A_i/2)$. The first term $\sim K_1 K_2$ describes the part of the excitonic system, which remains in the ground state $|g\rangle$ during both pulses. Accordingly, the corresponding phonon state also stays in its vacuum state $|0\rangle$. The second term $\sim K_1 S_2$ refers to the process, where the excitonic system is unaffected by the first pulse, but the second pulse excites the exciton. Due to the creation of an exciton, a coherent phonon state $|\beta(t)\rangle$ is generated. This process equals the one-pulse case. The third term, $\sim S_1 K_2$, describes the same situation, but now the first pulse excites the exciton and the second pulse does not affect the system. Thus, a coherent phonon $|\beta(t+\tau)\rangle$ is created at time $t = -\tau$. Finally, the forth term, $\sim S_1 S_2$, describes the state when both laser pulses change the electronic system. Therein, the first pulse excites the exciton and creates a coherent phonon $|\beta(t+\tau)\rangle$. At time $t = 0$, when the second pulse acts, the exciton is de-excited back to the ground state $|g\rangle$. This de-excitation can again be seen as a sudden shift of the equilibrium position of the harmonic oscillator potential back to the origin. However, when the second shift happens, the phonon state is in general not in its old equilibrium position, thus, its time dependence, but not its shape, is changed. In terms of displacement operators, the state $|\alpha(t)\rangle$ is created by

$$\begin{aligned}|\alpha(t)\rangle &= \hat{T}(\Gamma)\hat{D}[\tilde{\beta}(t)]\hat{D}[-\tilde{\beta}(t+\tau)]|\tilde{0}\rangle \\ &= e^{-i\Gamma^2 \sin(\omega_0\tau)}|\Gamma(e^{-i\omega_0 t} - e^{-i\omega_0(t+\tau)})\rangle, \end{aligned} \tag{34}$$

which is again a coherent state. The corresponding Wigner function $W_{\alpha(t)}$,

$$W_{\alpha(t)}(U,\Pi) = \frac{1}{2\pi}\exp\left\{-\frac{1}{2}[U-2\Gamma\left(\cos(\omega_0 t)-\cos(\omega_0(t+\tau))\right)]^2\right\} \times \exp\left\{-\frac{1}{2}[\Pi-2\Gamma\left(\sin(\omega_0(t+\tau))-\sin(\omega_0 t)\right)]^2\right\}, \tag{35}$$

is a two-dimensional Gaussian which moves on the circle $(\langle U\rangle,\langle\Pi\rangle) = (2\Gamma(\cos(\omega_0 t)-\cos(\omega_0(t+\tau))), 2\Gamma(\sin(\omega_0(t+\tau))-\sin(\omega_0 t))$. The circle center is the origin $(\bar{U},\bar{\Pi}) = (0,0)$.

With these ingredients we can write the full state of the system as

$$\begin{aligned}|\psi(t)\rangle = {} & K_1K_2|g,0\rangle + iK_1S_2e^{i(\phi_2-\tilde{\Omega}t)}|x,\beta(t)\rangle \\ & + iS_1K_2e^{i(\phi_1-\tilde{\Omega}(t+\tau))}|x,\beta(t+\tau)\rangle \\ & - S_1S_2e^{i(\phi_1-\phi_2-\tilde{\Omega}\tau)}|g,\alpha(t)\rangle.\end{aligned} \tag{36}$$

In the following we assume the case of an excitation with two $\pi/2$ laser pulses, such that $S_i = K_i = 1/\sqrt{2}$ and introduce the phase $\Phi = \phi_2 - \phi_1 + \tilde{\Omega}\tau$ to simplify the equations.

When we trace over the electronic variables in order to reduce the system to the phonon degrees of freedom we again obtain a statistical mixture for the reduced density matrix $\hat{\rho}_{ph}(t)$ of the phonon system

$$\begin{aligned}\hat{\rho}_{\mathrm{ph}}(t) = {} & \tfrac{1}{4}(|0\rangle - e^{-i\Phi}|\alpha(t)\rangle)(\langle 0| - e^{i\Phi}\langle\alpha(t)|) \\ & + \tfrac{1}{4}(|\beta(t)\rangle + e^{-i\Phi}|\beta(t+\tau)\rangle)(\langle\beta(t)| + e^{i\Phi}\langle\beta(t+\tau)|).\end{aligned} \tag{37}$$

We see that here a mixed state of two superposition states $|0\rangle + e^{-i\Phi}|\alpha(t)\rangle$ and $|\beta(t)\rangle + e^{-i\Phi}|\beta(t+\tau)\rangle$ is formed. Each superposition is formed by two coherent states. Such a superposition is called *cat state*.[11]

To illustrate this phonon state we again look at the corresponding Wigner function $W_{2\mathrm{pulse}}(U,\Pi)$. Again, the Wigner function is a sum of the two parts of the statistical mixture

$$W_{2\mathrm{pulse}} = \tfrac{1}{2}W_{0,\alpha(t)} + \tfrac{1}{2}W_{\beta(t),\beta(t+\tau)}. \tag{38}$$

Each part is the Wigner function of a cat state,

$$W_{0,\alpha(t)} = \tfrac{1}{2}\left\{W_0 + W_{\alpha(t)} - W^I_{[0,\alpha(t)]}\right\}, \tag{39}$$

which consists of the Wigner functions of the coherent states W_0 and $W_{\alpha(t)}$ and an interference term $W^I_{[0,\alpha(t)]}$. While the Wigner functions of the coherent states are two-dimensional Gaussians, the interference term has a different structure

$$\begin{aligned}W^I_{[0,\alpha(t)]}(U,\Pi) = {} & \frac{1}{\pi}\exp\left\{-\frac{1}{2}[U-\Gamma\left(\cos(\omega_0 t)-\cos(\omega_0(t+\tau))\right)]^2\right\} \\ & \times \exp\left\{-\frac{1}{2}[\Pi-\Gamma\left(\sin(\omega_0(t+\tau))-\sin(\omega_0 t)\right)]^2\right\} \\ & \times \cos\{\Gamma U[\sin(\omega_0 t)-\sin(\omega_0(t+\tau))] \\ & + \Gamma\Pi[\cos(\omega_0 t)-\cos(\omega_0(t+\tau))] + \Gamma^2\sin(\omega_0\tau) - \Phi\}.\end{aligned} \tag{40}$$

Still the first two exponential factors resemble a two-dimensional Gaussian, which moves concentrically to $W_{\alpha(t)}$ around (0,0) but with half the radius. This Gaussian is multiplied by a cosine-function, which changes the structure of this term qualitatively. As the cosine function oscillates around zero, it takes positive and negative values. Negative parts of the Wigner function are typically an indicator for quantum interferences, here associated with the quantum mechanical superposition.

Similarly, the second half of the two-pulse Wigner function can be decomposed into

$$W_{\beta(t),\beta(t+\tau)} = \tfrac{1}{2}\left\{W_{\beta(t)} + W_{\beta(t+\tau)} + W^I_{[\beta(t),\beta(t+\tau)]}\right\}, \tag{41}$$

where the Wigner functions of the coherent states $|\beta(t)\rangle$ and $|\beta(t+\tau)\rangle$ are given by Eq. (29). The interference term reads

$$\begin{aligned}W^I_{[\beta(t),\beta(t+\tau)]}(U,\Pi) = {} & \frac{1}{\pi}\exp\left\{-\frac{1}{2}[U-\Gamma\left(2-\cos(\omega_0(t+\tau))-\cos(\omega_0 t)\right)]^2\right\} \\ & \times \exp\left\{-\frac{1}{2}[\Pi-\Gamma(\sin(\omega_0 t)+\sin(\omega_0(t+\tau)))]^2\right\} \\ & \times \cos\{\Gamma U[\sin(\omega_0 t)-\sin(\omega_0(t+\tau))] \\ & + \Gamma\Pi[\cos(\omega_0 t)-\cos(\omega_0(t+\tau))] \\ & + \Gamma^2[2\sin(\omega_0(t+\tau)) - 2\sin(\omega_0 t) - \sin(\omega_0\tau)] - \Phi\}.\end{aligned} \tag{42}$$

Its structure is similar to the other interference term as it is composed of two Gaussian multiplied by a cosine function.

Coming back now to the full two-pulse Wigner function, we can decompose it into six terms, namely four two-dimensional Gaussians describing coherent states and two interference terms:

$$\begin{aligned}W_{2\mathrm{pulse}} = {} & \tfrac{1}{4}\left\{W_0 + W_{\alpha(t)} + W_{\beta(t)} + W_{\beta(t+\tau)}\right. \\ & \left. - W^I_{[0,\alpha(t)]} + W^I_{[\beta(t),\beta(t+\tau)]}\right\}\end{aligned} \tag{43}$$

One representative example for such a Wigner function is given in Fig. 3 for a time delay of $\tau = t_0/2$, a coupling constant of $\Gamma = 2$, and a phase of $\Phi = 0$. Having in mind that the Wigner function can be decomposed into six parts, we can easily understand its behavior. At $t = 0$ we see two Gaussians that were formed due to the first laser pulse. For $t > 0$ the two Gaussians each split into two Gaussians, such that four Gaussians are formed. The peaks of the Gaussians move on the sketched circles. Moreover, we can identify the two interference terms, which are structured by positive and negative stripes. They are found only on the axis between the pairs of Gaussians forming the cat states. The modulation with the cosine lies perpendicular to the connecting axis. When we look at the temporal behavior we see that the interference terms move corresponding to their attached Gaussians. $W^I_{[0,\alpha(t)]}$ moves concentrically to $\alpha(t)$. $W^I_{[\beta(t),\beta(t+\tau)]}$ lies on the center of the circle where both $W_{\beta(t)}$ and $W_{\beta(t+\tau)}$ are moving. There it rotates in time.

The corresponding probability distributions for the displacement $P(U)$ and momentum $P(\Pi)$ are shown in Fig. 4(a) as functions of time. Because the distributions are obtained from the Wigner function by integration, their behavior can be

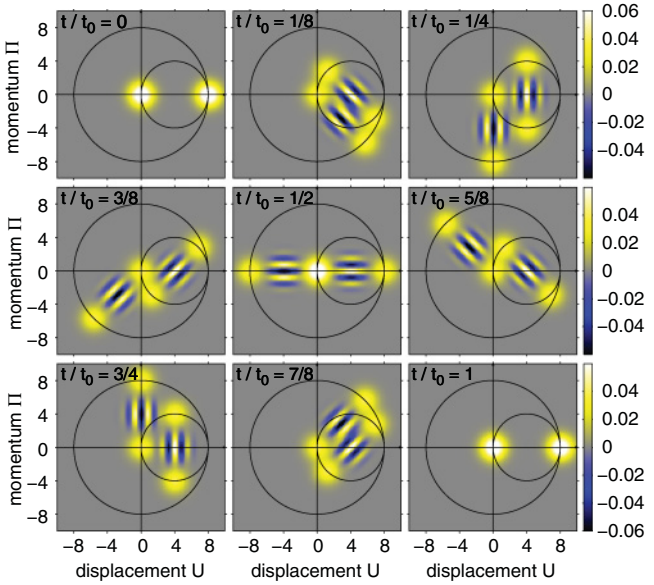

FIG. 3. (Color online) Series of snapshots of the two-pulse Wigner function $W_{2\text{pulse}}(U,\Pi)$ for a coupling constant $\Gamma = 2$. The circles depict the movement of the Gaussians corresponding to the coherent states.

easily understood by looking at the Wigner function. At $t = 0$ the distribution for the displacement $P(U)$ exhibits two peaks corresponding to the two Gaussians in the Wigner functions. Then the Gaussians move together, and at $t/t_0 = 1/4$ many peaks appear in $P(U)$, as now the integral over two Gaussians and one interference term is performed. When for certain U the interference terms have negative values (at the blue areas), the integral over the Gaussian is canceled by the integral over the interference term and thus $P(U)$ is zero. If the interference term is positive, $P(U)$ is increased. At $t/t_0 = 1/2$, three peaks are observed, with the strength of the middle peak being twice as high as the strength of the outer peaks. The middle peak is formed by integrating over two Gaussians, namely W_0 and $W_{\beta(t+\tau)}$, while the outer peaks are the results of the integral over one Gaussian each. The integrals over the interference terms are zero as positive and negative values cancel each other and, thus, in between the peaks the probability distribution is zero. The distribution $P(U)$ at $t/t_0 = 3/4$ looks the same as at $t/t_0 = 1/4$, but now minima and maxima are inverted, in agreement with the Wigner function. The mean value $\langle U \rangle$ can be easily deduced to oscillate in time. In the same way we can understand the behavior of $P(\Pi)$.

Let us now turn to the question of whether, in this case, the phonon system exhibits squeezing. For this purpose we look at the EIF S_u and S_π, which are depicted in Fig. 4(b). In agreement with the probability distributions, we find that the EIF are oscillating in time. For $t/t_0 = 0,1/2,1$, S_u is large as the Wigner function is spread out along the displacement axis, while at $t/t_0 = 1/4,3/4$, S_u is small because the Wigner function is outspread along the momentum axis. The EIF of the momentum S_π exhibit the reverse behavior. Still, for all times, the EIF are above or equal to zero, thus, no squeezing occurs.

From quantum optics it is known that a single cat state can exhibit squeezing for certain parameters,[11] because the interference term can lead to a reduced variance, i.e., to a squeezed state. This only holds when the amplitudes of the involved coherent states are small enough such that the

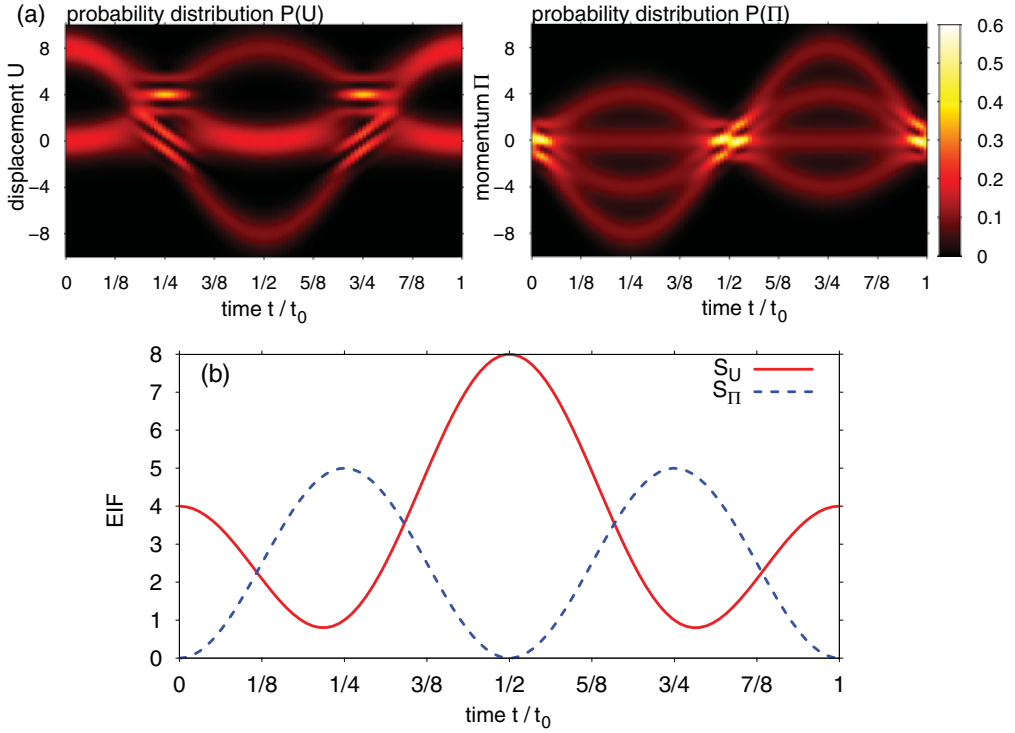

FIG. 4. (Color online) (a) Contour plot of the probability distributions $P(U)$ and $P(\Pi)$ as function of times. (b) EIF S_u and S_π. The coupling constant is $\Gamma = 2$.

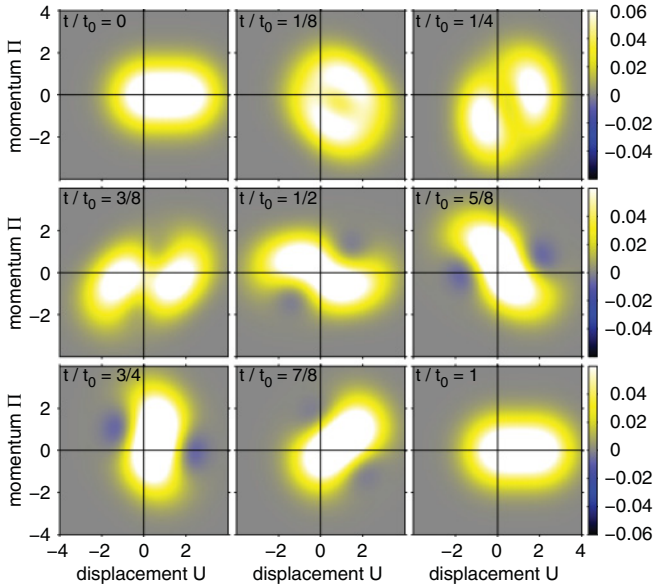

FIG. 5. (Color online) Series of snapshots of the two-pulse Wigner function $W_{\mathrm{2pulse}}(U,\Pi)$ for a coupling constant $\Gamma = 0.5$.

interference term overlaps with the Gaussians, which is not the case in Fig. 3. Furthermore, the relative phase of the cat state, here given by Φ, determines whether squeezing occurs or not. In a previous work[10] we found most pronounced squeezing for a phase $\Phi = \pi/2$. The coupling constant $\Gamma = 0.5$ has been found to be optimal in terms of very low variances.

Snapshots of the Wigner function obtained for the same excitation conditions as above but for a coupling constant $\Gamma = 0.5$ and a phase $\Phi = \pi/2$ are shown in Fig. 5. A decrease of the coupling constant leads to a reduction of the radii of the circles as well as to a movement of the center of the β circle closer to the origin. However, the widths of the Gaussians and interference terms remain the same. Therefore, in Fig. 5 the constituents of the Wigner function cannot be resolved anymore. While most of the time the Wigner function is only positive, at certain times, e.g., at $t/t_0 = 3/4$, clearly negative parts of the Wigner function can be seen. Indeed, at this time the Wigner function looks narrower than the typical Gaussian. If we look at the probability distributions $P(U)$ and $P(\Pi)$ shown in Fig. 6(a) and compare them to the Wigner function, their time behavior can be easily understood. At $t/t_0 = 1/4$ we see two bumps in the Wigner function, which correspond to the two broad peaks in $P(U)$. In contrast at $t/t_0 = 3/4$, the Wigner function is elongated along the Π axis and correspondingly $P(U)$ is narrow.

To see whether this state exhibits squeezing, the fluctuations are plotted in Fig. 6(b). Indeed, at times around $t/t_0 = 3/4$, we find that S_u is negative. In agreement with the probability distribution $P(U)$, the fluctuations are large at $t/t_0 = 1/2$. The fluctuations of the momentum S_π also fall below zero around the times $t/t_0 = 1/2$ and $t/t_0 = 1$. Thus, the phonons exhibit squeezing for these parameters.

We have found that by reducing the coupling constant, the Gaussians and interference terms of the Wigner function overlap and, thus, by the negative parts of the interference terms the Wigner function can become narrower. This results in a narrower probability density and reduced fluctuations compared to the vacuum state. If we reduce the coupling constant further, this still holds as we have shown in previous

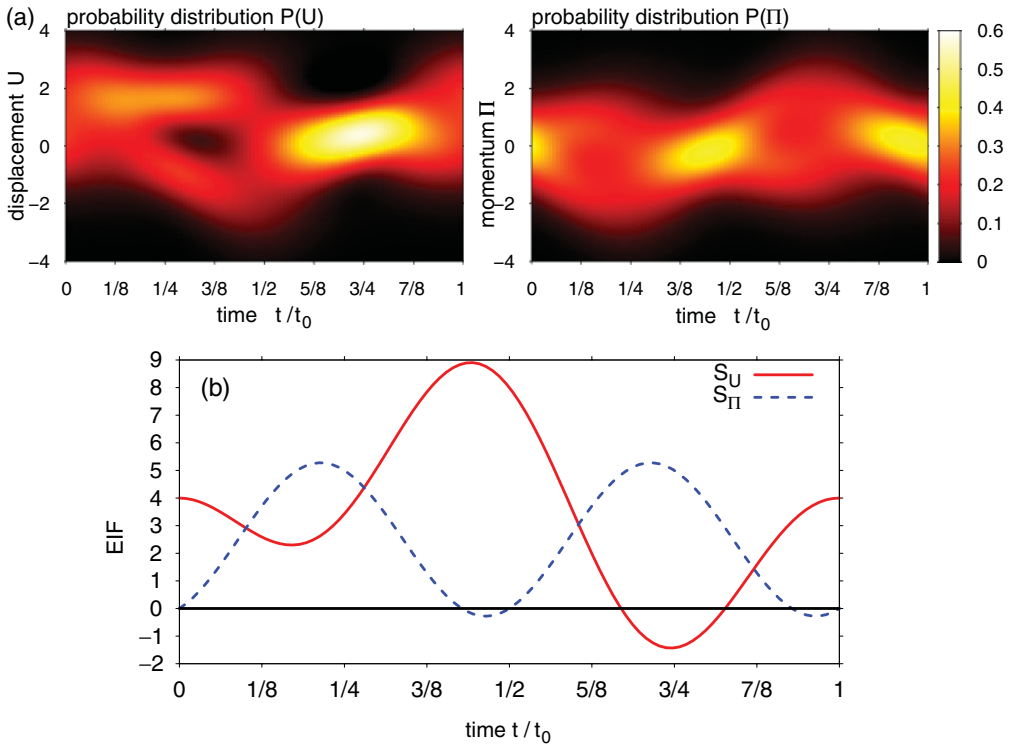

FIG. 6. (Color online) (a) Contour plot of the probability distributions $P(U)$ and $P(\Pi)$ as function of time and (b) corresponding EIF S_u and S_π.

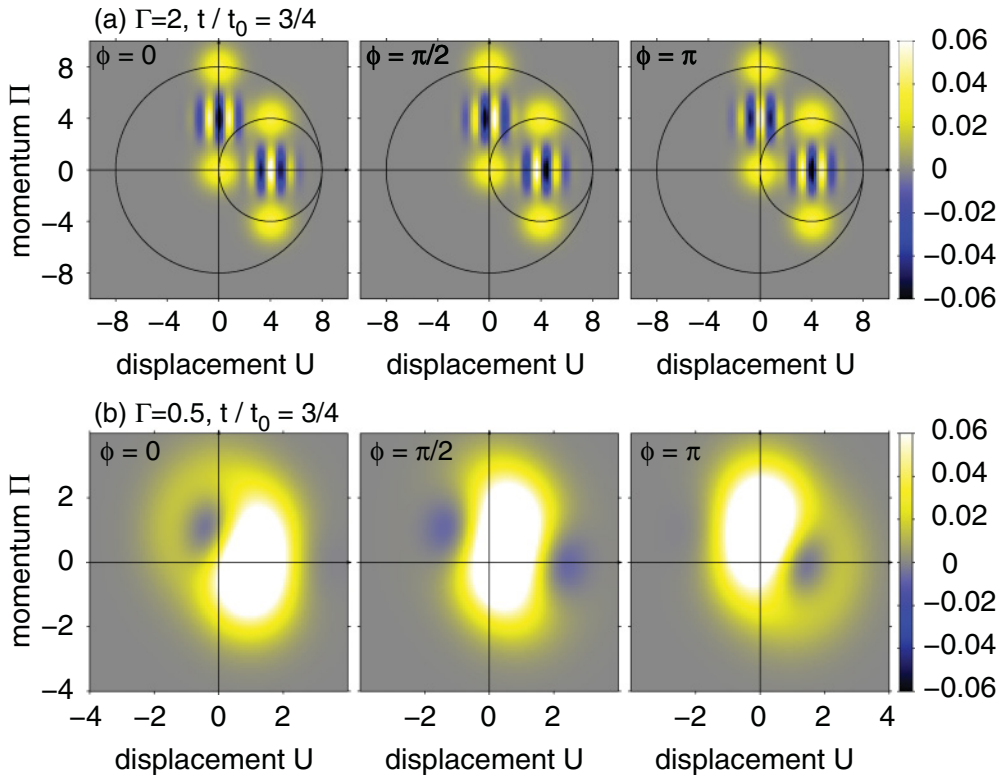

FIG. 7. (Color online) Snapshots of the Wigner function at time $t/t_0 = 3/4$ for different phases $\Phi = 0,\pi/2,\pi$ at a coupling constant of (a) $\Gamma = 2$ and (b) $\Gamma = 0.5$.

studies[10] for $\Gamma = 0.03$. We have also found that the squeezing is most pronounced for a phase $\Phi = \pi/2$ and that no squeezing occurs when $\Phi = 0$. To understand the influence of the phase, we analyze the influence of the phase on the Wigner function and the resulting probability distributions in more detail. For this purpose, in Fig. 7(a) we have plotted snapshots at $t/t_0 = 3/4$ of the Wigner function for a coupling constant of $\Gamma = 2$ and for different phases $\Phi = 0,\pi/2$, and π. The only terms that depend on the phase Φ are the interference terms W^I, as can be seen from Eqs. (40) and (42). When we compare the three different phases, we find that the maxima and minima of the cosine function shift according to the phase. Let us, for example, look at the interference part at $U = 0$: for $\Phi = 0$ there is a minimum at $U = 0$, while for $\Phi = \pi/2$ there is a node and for $\Phi = \pi$ there is a maximum. The situation is reversed at $U = 2\Gamma = 4$: in this case for $\Phi = 0$ there is a maximum at $U = 4$, for $\Phi = \pi/2$, there is a node and for $\Phi = \pi$ there is a minimum. We have seen that the probability distribution $P(U)$ strongly depends on the interference terms and can be either narrower or broadened, depending on the precise position of their negative parts.

When we look at the coupling constant $\Gamma = 0.5$ [Fig. 7(b)], where squeezing is possible, the influence of the phase becomes clear. For $\Phi = \pi/2$, the Wigner function is elongated along the Π axis while interference minima on both sides lead to a narrowing in the U direction. Consequently, squeezing in the displacement is found. For $\Phi = 0$ and $\Phi = \pi$, on the other hand, a minimum due to the interference terms is seen only on one side. It does not lead to a narrowing of the Wigner function. For these phases, no squeezing occurs.[10]

In our study we have so far not considered dephasing or relaxation processes induced, e.g., by the coupling of the exciton or the LO phonons to acoustic phonons. Let us, therefore, briefly comment on these phenomena. LO phonons have a finite lifetime, which is typically limited by the anharmonic decay into acoustic or lower lying optical phonons. For typical zincblende-type materials the LO phonon lifetime is typically in the range of 5–10 ps.[33–35] LO phonon energies in the range of 20–40 meV imply phonon oscillation periods in the range of 100–200 fs. Thus, at least 25 oscillations can take place before the LO phonons will decay. The pure dephasing of the exciton, on the other hand, typically leads to an initial decay of the interband coherence on a time scale of about 500–1000 fs.[21] However, this process only limits the maximal time between the two laser pulses, which in our case is less than a single LO phonon period and, thus, much shorter than the characteristic pure dephasing time.

IV. CONCLUSIONS

In conclusion, we have studied the phonon dynamics and fluctuations of lattice displacement and momentum of a quantum dot after excitation with ultrafast laser pulses. The quantum states of the generated phonons have been represented with the help of the Wigner function. After the excitation with a single laser pulse, the electronic and phononic system become entangled. The Wigner function of the phonons is the sum of two Gaussians, one corresponding to the vacuum state and one to the coherent phonon state, which is generated

during the excitation. Accordingly the fluctuations of the phonon variables show an oscillatory behavior; however, no squeezing occurs. For the excitation with two laser pulses, the entanglement between electronic and phononic system leads to a more complicated structure of the Wigner function, where four Gaussians corresponding to four different coherent states as well as two interference terms appear. Because the interference terms can take negative values, the probability distributions for the displacement and the momentum can become narrower than the vacuum distributions and squeezing is found. The dependence on the phase is crucial as it determines the position of the negative parts of the interference terms. When the coupling becomes too strong, squeezing cannot occur as the interference terms do not overlap with the Gaussians any more. The Wigner function thus provides a very intuitive picture to understand the phonon dynamics and the origin of squeezing for certain excitation conditions and material parameters.

[1] S. L. Johnson, P. Beaud, E. Vorobeva, C. J. Milne, É. D. Murray, S. Fahy, and G. Ingold, Phys. Rev. Lett. **102**, 175503 (2009).

[2] O. V. Misochko, K. Kisoda, K. Sakai, and S. Nakashima, Appl. Phys. Lett. **76**, 961 (2000).

[3] O. V. Misochko, K. Sakai, and S. Nakashima, Phys. Rev. B **61**, 11225 (2000).

[4] G. A. Garrett, A. G. Rojo, A. K. Sood, J. F. Whitaker, and R. Merlin, Science **275**, 1638 (1997).

[5] A. Bartels, T. Dekorsy, and H. Kurz, Phys. Rev. Lett. **84**, 2981 (2000).

[6] X. Hu and F. Nori, Phys. Rev. B **53**, 2419 (1996).

[7] X. Hu and F. Nori, Phys. Rev. Lett. **76**, 2294 (1996).

[8] A. Hussain and S. R. Andrews, Phys. Rev. B **81**, 224304 (2010).

[9] D. F. Walls, Nature (London) **306**, 141 (1983).

[10] S. Sauer, J. M. Daniels, D. E. Reiter, T. Kuhn, A. Vagov, and V. M. Axt, Phys. Rev. Lett. **105**, 157401 (2010).

[11] C. C. Gerry and P. Knight, *Introductory Quantum Optics* (Cambridge University Press, New York, 2005).

[12] W. P. Schleich, *Quantum Optics in Phase Space* (Wiley-vch, Berlin, 2001).

[13] J. M. Daniels, T. Papenkort, D. E. Reiter, T. Kuhn, and V. M. Axt, Phys. Rev. B **84**, 165310 (2011).

[14] X. Hu and F. Nori, Phys. Rev. Lett. **79**, 4605 (1997).

[15] V. Buzek and P. L. Knight, Opt. Commun. **81**, 331 (1991).

[16] J. Janszky and A. V. Vinogradov, Phys. Rev. Lett. **64**, 2771 (1990).

[17] V. V. Dodonov, I. A. Malkin, and V. I. Man'Ko, Physica **72**, 597 (1974).

[18] B. Yurke and D. Stoler, Phys. Rev. Lett. **57**, 13 (1986).

[19] C. Kurtsiefer, T. Pfau, and J. Mlynek, Nature (London) **386**, 150 (1997).

[20] A. Ourjoumtsev, H. Jeong, R. Tualle-Brouri, and P. Grangier, Nature (London) **448**, 784 (2007).

[21] A. Vagov, V. M. Axt, T. Kuhn, W. Langbein, P. Borri, and U. Woggon, Phys. Rev. B **70**, 201305 (2004).

[22] K. J. Yee, K. G. Lee, E. Oh, D. S. Kim, and Y. S. Lim, Phys. Rev. Lett. **88**, 105501 (2002).

[23] Y. S. Lim, S. C. Yoon, K. J. Yee, Y. H. Ahn, E. Oh, and J. H. Lee, Appl. Phys. Lett. **82**, 2446 (2003).

[24] Y. Kasai, D. Suzuki, H. Kunugita, and K. Ema, J. Lumin. **129**, 1820 (2009).

[25] G. C. Cho, W. Kütt, and H. Kurz, Phys. Rev. Lett. **65**, 764 (1990).

[26] A. Vagov, V. M. Axt, and T. Kuhn, Phys. Rev. B **66**, 165312 (2002).

[27] V. M. Axt, T. Kuhn, A. Vagov, and F. M. Peeters, Phys. Rev. B **72**, 125309 (2005).

[28] T. Stauber, R. Zimmermann, and H. Castella, Phys. Rev. B **62**, 7336 (2000).

[29] D. E. Reiter, D. Wigger, J. M. Daniels, T. Papenkort, A. Vagov, V. M. Axt, and T. Kuhn, Phys. Status Solidi B **248**, 825 (2011).

[30] B. Krummheuer, V. M. Axt, and T. Kuhn, Phys. Rev. B **65**, 195313 (2002).

[31] B. Krummheuer, V. M. Axt, T. Kuhn, I. D'Amico, and F. Rossi, Phys. Rev. B **71**, 235329 (2005).

[32] V. I. Klimov, S. A. Ivanov, J. Nanda, M. Achermann, I. Bezel, J. A. McGuire, and A. Piryatinski, Nature (London) **447**, 441 (2007).

[33] A. R. Bhatt, K. W. Kim, and M. A. Stroscio, J. Appl. Phys. **76**, 3905 (1994).

[34] X. Q. Li and Y. Arakawa, Phys. Rev. B **57**, 12285 (1998).

[35] F. Vallée, Phys. Rev. B **49**, 2460 (1994).